Simplified Approaches to Design Medium-Rise Unbraced Steel Storage Pallet Racks. I: Elastic Buckling Analysis

Claudio Bernuzzi[1]; Armando Gobetti[2]; Giammaria Gabbianelli[3]; and Marco Simoncelli[4]

Introduction

Industrial steel storage pallet racks (Fig. 1) are composed of a regular sequence of upright frames, i.e., built-up laced members, which are connected to one other in the downaisle direction by pairs of horizontal beams (pallet beams) sustaining pallet units. The need to optimize rack performance in terms of stored goods and products generally hampers the arrangement of bracing systems in the downaisle direction. Stability against lateral loads is thus provided by the flexural continuity associated with beam-to-column joints and base-plate connections. Racks are considered nonbuilding structures, i.e., self-supporting structures that carry gravity loads supported by the earth or other structures (Shafer 2011; Godley 1991). They are very similar to the framed steelworks traditionally used for civil and commercial buildings even though there are great differences in the geometry of the members and types of joints used to connect members. The need to minimize the weight of the uprights and other components results in forming intermediate cross section stiffeners, allowing the use of members with limited thickness, which is generally between 1.5 and 3 mm. Rack design is generally quite complex. The performances of uprights are governed by the interaction between local and distortional buckling (Dinis et al. 2013). Moreover, the presence of nonlinear semirigid beam-to-column connections offering limited values of flexural continuity (Baldassino and Bernuzzi 2000), nonnegligible influence of second-order effects, and geometrical and mechanical imperfections do not allow design on the basis of pure theoretical approaches (Baldassino and Zandonini 2011).

Furthermore, the most commonly used upright cross sections are characterized by the presence of one axis of symmetry and the shear center does not often coincide with the centroid. As a consequence, warping torsion and direct interaction between bending and torsion (Chen and Atsuta 1977), which are usually neglected in routine design, play a fundamental role in rack response. Most advanced rack design provisions have been very recently updated for Europe {EN 15512 [European Committee for Standardization (CEN) 2009]}, United States [Rack Manufacturers Institute (RMI) 2012], and Australia [AS 4084 (Australian Standards 2012)], but further improvements are necessarily required to increase their level of safety. Currently, inadequate attention has been paid to the key features associated with the single symmetry of the cross section uprights. The approaches currently adopted for routine design are inappropriate and inadequate in some instances because they are

[1]Associate Professor, Dept. of Architecture, Built Environment and Construction Engineering, Politecnico di Milano, Piazza Leonardo da Vinci, 32, 20133 Milano, Italy.

[2]Associate Professor, Dept. of Civil Engineering and Architecture, Università di Pavia, Via A. Ferrata, 3, 27100 Pavia, Italy.

[3]Ph.D. Student, Dept. of Civil Engineering and Architecture, Università di Pavia, Via A. Ferrata, 3, 27100 Pavia, Italy (corresponding author). E-mail: giammaria.gabbianelli@gmail.com

[4]Ph.D. Student, Dept. of Architecture, Built Environment and Construction Engineering, Politecnico di Milano, Piazza Leonardo da Vinci, 32, 20133 Milano, Italy.

Note. This manuscript was submitted on February 22, 2014; approved on January 7, 2015; published online on March 5, 2015. Discussion period open until August 5, 2015; separate discussions must be submitted for individual papers. This paper is part of the ***Journal of Structural Engineering***, © ASCE, ISSN 0733-9445/04015036(11)/$25.00.

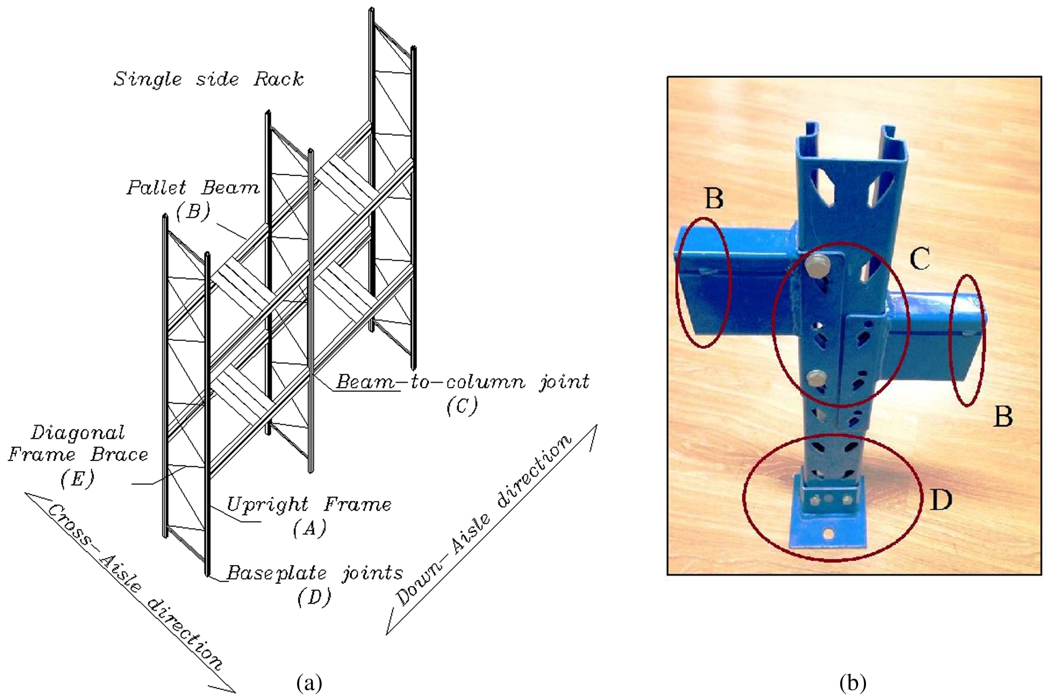

Fig. 1. Typical selective pallet rack: (a) most common definitions; (b) detail of end upright

directly derived from the ones proposed for structures composed of doubly symmetric cross section members.

Teh et al. (2004) focused their attention on a double-sided high-rise steel pallet rack frame and demonstrated that the beam elements available in most commercial finite-element (FE) frame analysis programs, which neglect cross section warping and shear-center eccentricity, are not sufficiently accurate for buckling analyses of rack frames composed of singly symmetric open cross sections. Similar studies were conducted by Gilbert and Rasmussen (2012), which considered the warping torsion for uprights in drive-in pallet rack structures, calibrating finite-element models with an experimental test. As an alternative to the use of the beam element, Sangle et al. (2012) and Bajoria et al. (2010) carried out extensive numerical researches on pallet racks through very refined finite-element models using shell elements to simulate uprights, beams, and connections. However, this modeling technique does not appear suitable for routine rack design because each load case requires a separate arrangement of the mesh and a new analysis of the output data.

This paper is the first part of a two-part paper and deals with the design for static loading of unbraced racks and, in particular, prediction of the elastic critical load for the sway mode. To this purpose, rack codes allow simplified calculations on the basis of Horne's method (Horne 1975) as for the more traditional steel-framed systems. To evaluate the accuracy of these simplified methods when applied to steel storage pallet racks, a numerical analysis has been carried out. In particular, an open source finite-element program for academic use (*Śiva*) (Bernuzzi and Gobetti 2014), developed from the original *NONSAP* (Bathe et al. 1978) has been improved, implementing suitable routines for buckling analysis and second-order effects. More recently, the need to allow a rack structural analysis led to further development of the program by adding both a rotational spring model and a suitable beam element formulation for a singly symmetric cross section.

This paper studies six medium-rise rack frames, which differed for the geometries of the whole frame and its components, which have been selected from standard products designed in accordance with the European Standard EN 15512 (CEN 2009). For each of them, a parametric analysis has been carried out by varying the degree of the rotational stiffness of both beam-to-column joints and base-plate connections. Finally, a safety factor is proposed to be used when a critical load multiplier is on the basis of the finite-element analysis packages, which neglect the presence of singly symmetric cross section members. Simplified approaches for seismic design are discussed and applied in the companion paper (Bernuzzi et al. 2015a).

Rack Analysis Models

The thin-walled beam theory was well-established by Vlasov (1961) and Timoshenko and Gere (1961) for isolated members with a singly symmetric cross section. The outcomes of these studies are nowadays available for structural engineers, especially with reference to equations governing the overall response, prediction of the elastic buckling loads of beams and columns, and approaches to define the complex distribution of normal and tangential cross section stresses. With regard to complete racks, owing to the complexity of these structural systems, some key features of the behavior of their components are currently neglected or not adequately considered in routine design. Structural analysis is carried out through FE methods by using beam element formulations on the basis of six degrees of freedom (DOFs) per node, which have been proposed and correctly used for members having two axes of symmetry (Bathe and Wilson 1976; Hughes 1987), i.e., when the shear center coincides with the cross section centroid. For each beam node, three displacements (u, v, and w) and three rotations (φ_x, φ_y, and φ_z) are used in the FE analysis [Fig. 2(a)] to evaluate the set of displacements and internal forces and moments required to execute all of the design verification checks. Furthermore, overall buckling load is usually determined by considering only the flexural buckling modes, i.e., the ones able to be captured via six-DOF beam formulations. Design procedures in accordance with European and United States rack codes relegate warping influence only to the flexural torsional buckling of columns and beam columns,

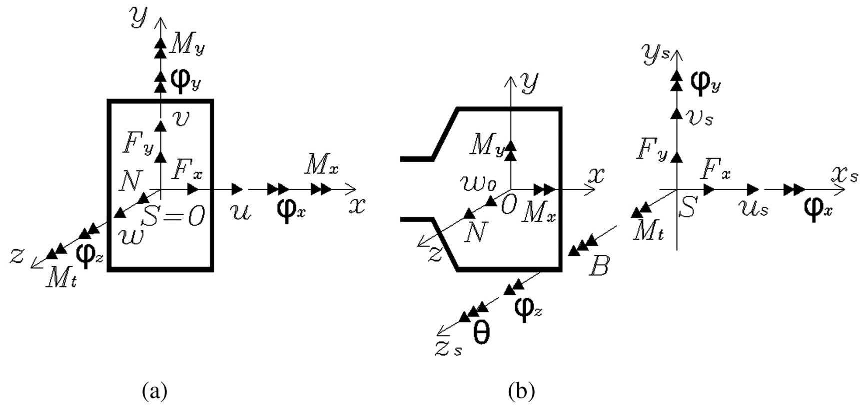

Fig. 2. Displacements, internal forces, and moments at node location for FE beam formulation: (a) six DOFs; (b) seven DOFs

which has to be verified with regard to isolated members of an appropriate buckling length. As a consequence, internal forces and torsional and bending moments are evaluated, neglecting warping effects, with the result that the frame deformability to horizontal loads is underestimated, as is the safety, with reference to both cross section resistance (Bernuzzi et al. 2014a) and member stability (Bernuzzi et al. 2014b, 2015b).

Suitable beam formulations accounting for warping have already been proposed in the literature (Hsiao and Lin 2000; Turkalj et al. 2003; Werkle 2008) and are now implemented in a few FE general purpose analysis programs, e.g., *Abaqus* (Hibbit, Karlsson and Sorensen 2006), *LS-DYNA*, *SOFiSTiK* (2013), and *ConSteel 7.0* (ConSteel Solutions 2010). Owing to the noncoincidence between the shear center S and the centroid O, in the case of singly symmetric cross sections, reference is generally made to Point S for the definition of all of the displacements, except for the axial displacement w_O, which is assumed in correspondence to Point O. Shear forces (F_x and F_y), uniform torsional moment (M_t), and bimoment (B) are referred to Point S, whereas bending moments (M_x and M_y) and axial force (N) are defined with respect to the centroid [Fig. 2(b)]. Cross section warping θ, i.e., the seventh DOF, which is essential to correctly model open singly symmetric cross section members, is defined as

$$\theta = \theta(z) = -\frac{d\varphi_z}{dz} \tag{1}$$

Only the presence of θ guarantees that the rack design is developed using appropriate analysis tools and by adequately considering the key features of rack uprights.

As previously discussed, racks are regular structural systems, and in the present study, attention has been focused on typical medium-rise racks, which were unbraced in the downaisle direction. In particular, reference is made to three rack uprights (identified in the following as $M\_$, $G\_$ and $T\_$), which differed for the cross section geometries (Fig. 3) and were selected to be sufficiently representative for routine design cases. For each upright, the ratio between the second moments of area (I_x/I_y), major and minor section modulus ($W_x/W_{y,\mathrm{sup}}$ and $W_x/W_{y,\mathrm{inf}}$), and radii of gyration (ρ_x/ρ_y) are reported in Table 1, together with the ratio x_O/d, i.e., shear center eccentricity (x_O), with respect to the centroid over the distance (d) between the centroid and the middle line of the web. The "Appendix" of the companion paper (Bernuzzi et al. 2015a) provides all of the computations associated with the considered simplified approaches applied to a two-bay and four-load level rack for research replication purposes. The mechanical and geometrical data of members and joints are reported together with all of the analysis results related to the use of both six- and seven-DOF FE beam formulations.

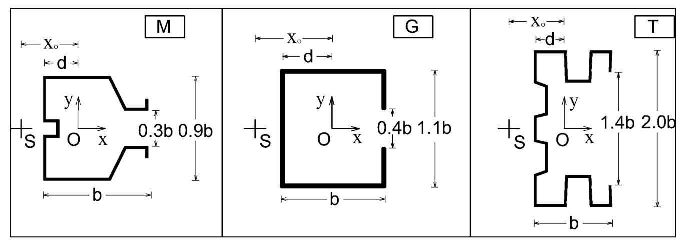

Fig. 3. Geometry of cross sections considered in present study

Table 1. Key Data of the Considered Upright Cross Sections

Section properties	*M* section	*G* section	*T* section
I_x/I_y	0.992	1.393	4.709
ρ_x/ρ_y	0.996	1.180	2.170
$W_x/W_{y,\mathrm{sup}}$	1.234	1.357	2.901
$W_x/W_{y,\mathrm{inf}}$	0.838	1.113	1.891
x_O/d	2.306	2.996	1.989

The selected cross sections have significantly different geometric properties, as it appears immediately by considering the values of I_x/I_y, which approximately range from 1.0 to 4.7, and x_O/d, which is approximately 2.0–3.0. These differences directly reflect the values of the elastic buckling axial load. In the case of a singly symmetric cross section that is similar to the ones presented in Fig. 3, the coupling between bending and compression could lead to a flexural-torsional buckling load ($N_{\mathrm{cr,FT}}$) that is significantly lower than the flexural one ($N_{\mathrm{cr},F}$), which is contrary to what occurs in the case of doubly symmetric cross section members, in which the flexural buckling is dominant to the torsional buckling.

As to the rack geometry, reference has been made to four ($M\_$ racks) or six ($T\_$ and $G\_$ racks) bay pallet racks unbraced in the downaisle direction, and the depth of the upright frame is equal to 1.00 m for $M\_$ and $G\_$ racks and 1.04 m for $T\_$ racks, as it appears in Fig. 4. A total of two rack configurations for the downaisle direction have been considered for each upright type, which differed in the number of load levels. The $M\_$ and $G\_$ uprights are associated with typical V and Z upright frame panels, respectively, whereas for $T_$racks, the more traditional cross-braced X panels, with diagonals resisting to both tension and compression, in the upright frame guarantee the stability in the cross-aisle direction. Table 2 shows the key data of the racks considered in the numerical analysis in terms of beam span (L_b), interstory height (h_{LL}), total height (H_{tot}),

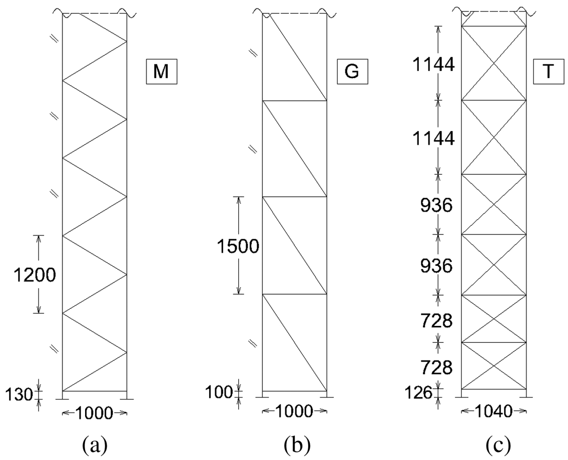

Fig. 4. Upright frames (dimensions in millimeters): (a) M_racks; (b) G_racks; (c) T_racks

number of load levels (N_{LL}), and height of the upright panel frame (h_u). For each upright, the case of four load levels has always been considered. In addition, for the G_ and T_ racks and M_racks, three and five load levels, respectively, have also been included in the parametric study. As to the other rack components, Table 2 displays their details. Pallet beams are realized by means of rectangular hollow square sections (RHSs). As to the lacings of the upright frames, square hollow sections (SHSs) for M_ and G_ racks and circular hollow sections (CHSs) for T_ racks have been used. All of the rack components have been considered to belong to Class 3 [EN 1993-1-1 (CEN 2005b)], i.e., unable to develop plasticity but not characterized by the presence of local and distortional buckling. The decision to adopt this assumption aims to focus attention only on a few key parameters, owing to both the main scopes of the research and the need to limit the number of variables influencing research outcomes. As to the load conditions, the sole case of fully loaded racks was considered, with pallet units interested by a uniform distributed load on pallet beams. Overall, frame imperfections equal to 0.0033 rad in terms of out of plumb (ϕ) of the uprights in both the cross-aisle and downaisle directions have been considered jointly by simulating the horizontal forces concentrated on each floor level. For each of these six racks, attention has been focused on the following parameters:

- The degree of flexural stiffness associated with beam-to-column joints. The elastic rotational stiffness of beam-to-column joints, $S_{j,\text{btc}}$, was defined on the basis of the classification criteria of Part 1-8 of Eurocode 3 (EC3) [EN 1993-1-8 (CEN 2005c)]. In particular, few values of $S_{j,\text{btc}}$ of interest for practical application (Baldassino and Bernuzzi 2000) have been identified as a multiple (by means of the term $\rho_{j,\text{btc}}$) of the reference stiffness value $S_{j,\text{btc}}^{\text{EC3-LB}}$ defined as

$$S_{j,\text{btc}} = \rho_{j,\text{btc}} \cdot S_{j,\text{btc}}^{\text{EC3-LB}} \tag{2a}$$

where $S_{j,\text{btc}}^{\text{EC3-LB}}$ = rotational stiffness associated with the lower bound of the semirigid domain, i.e., the value corresponding to the transition between the flexible and semirigid joint regions, which is defined as

$$S_{j,\text{btc}}^{\text{EC3-LB}} = 0.5 \frac{E \cdot I_b}{L_b} \tag{2b}$$

where E = Young's modulus; and I_b and L_b = second moment of area and length of the beam, respectively.

Parameter $\rho_{j,\text{btc}}$ ranges from 0.5 to 10.0. The lowest values are the ones obtained from tests on typical boltless connections, whereas the greatest values are experimentally obtained on the same connections by inserting one or two bolts in the bracket at the beam ends to increase joint seismic performances, especially in terms of stiffness, ductility, and energy absorption capabilities.
- The degree of flexural stiffness associated with base-plate connections. As stated in the European provisions for the connection design [EN 1993-1-8 (CEN 2005c)], the rotational stiffness $S_{j,\text{base}}^{\text{EC3-UB}}$ at the boundary between the semirigid and rigid joint regions can be assumed as

$$S_{j,\text{base}}^{\text{EC3-UB}} = 30 \frac{E \cdot I_u}{h_{\text{LL}}} \tag{3}$$

where I_u = second moment of area of the upright cross section for flexure in the downaisle direction; and h_{LL} = distance from the foundation to the first load level.

As in the case of beam-to-column joints, the values of the rotational stiffness $S_{j,\text{base}}$ have also been selected as a multiple by the term $\rho_{j,\text{base}}$ of the reference stiffness $S_{j,\text{base}}^{\text{EC3-UB}}$ for base-plate connections as

$$S_{j,\text{base}} = \rho_{j,\text{base}} \cdot S_{j,\text{base}}^{\text{EC3-UB}} \tag{4}$$

In this paper, three different values for $\rho_{j,\text{base}}$ have been considered for base-plate connections, i.e., 0.15, 0.30, and 0.45, respectively, which are typical of the considered upright bases, despite the fact that in several studies, the column bases have been modeled as the ideal restraints of hinged and fixed bases (Filiatrault et al. 2006; Bernuzzi et al. 2014a), which are very rarely guaranteed by commercial base-plate connections (Baldassino and Bernuzzi 2000). Fig. 5 displays the layout of the executed analysis and explains the symbols used to discuss the research outcomes.

In accordance with European practice, thick brackets are generally welded to the beam ends and lacings are bolted in the oversized holes in the upright flanges. As a consequence, warping has been considered free at the top and fixed at the bottom of the uprights and fixed at the beam ends and free at the lacing ends of the upright frames.

Table 2. Key Data of the Considered Rack Frames

	Downaisle direction					Cross-aisle direction		
Racks	L_b (m)	Beam pallets section	h_{LL} (m)	H_{tot} (m)	N_{LL}	Type of brace	Upright type	h_u (m)
M_4	2.78	RHS 160 × 40 × 1.3	1.80	7.20	4	SHS 30 × 30 × 3	M	1.20
M_5	2.78		1.20	6.30	5			1.20
G_3	2.60	RHS 100 × 50 × 3.0	2.00	6.10	3	SHS 30 × 30 × 3	G	1.50
G_4	2.60		1.50	6.10	4			1.50
T_3	2.83	RHS 165 × 40 × 2.0	2.50	8.25	3	CHS $d = 30$; $t = 1.5$	T	0.73
T_4	2.83		1.97	8.25	4			0.73

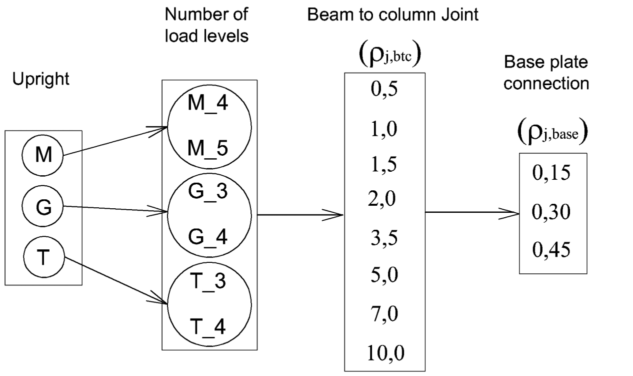

Fig. 5. Synopsis of numerical cases considered in parametric analysis

As previously discussed, FE analysis has been executed by *Śiva* software (C. Bernuzzi and A. Gobetti, "An innovative finite element formulation for analysis of beam element with thin-walled mono-symmetric section," submitted, *Costruzioni Metalliche*), which is a FE analysis program for academic use that was suitably modified by the authors and derived from *NONSAP* (Bathe et al. 1978). In addition to the beam formulation with seven DOFs, *Śiva*'s library offers the more traditional beam element on the basis of the classical six-DOF beam formulation, and both formulations have been used for the numerical study.

Prediction of the Elastic Sway Buckling

The first step of each routine calculation for any steel structural design under a static load is represented by the choice of the analysis methods, which is selected on the basis of the overall flexibility to lateral loads. Internal forces and moments are consequently evaluated by means of an elastic analysis, which in the case of unbraced steel frames can be of the first or second order. From a practical point of view, this very important choice is associated with the value of the elastic critical load multiplier α_{cr}, which is defined as the ratio between the elastic critical buckling load for the global instability sway mode (V_{cr}) and the total design vertical load of the structure (V_{Ed}), i.e., $\alpha_{cr} = V_{cr}/V_{Ed}$. In particular, the most recently updated rack standards EN 15512 (CEN 2009) and AS 4084 (Australian Standards 2012) recommend that if $\alpha_{cr} \geq 10$ or, equivalently, $V_{Ed}/V_{cr} \leq 0.1$, the rack is classified as a nonsway frame. A first-order analysis is more than adequate for design purposes. On the contrary, if $\alpha_{cr} \leq 10$ or, equivalently, $V_{Ed}/V_{cr} \geq 0.1$, the rack behaves as a sway frame, and second-order effects have to be considered in the structural analysis. Appropriate nonlinear FE formulations are hence strongly recommended to also accurately predict the frame response in the case of large displacements (large deflection analysis should be required). When $3.33 \leq \alpha_{cr} \leq 10$ or, equivalently, if $0.1 \leq V_{Ed}/V_{cr} \leq 0.3$, the structural analysis has to account for second-order effects, but the use of simplified approaches, such as the amplified sway moment method [EN 15512 (CEN 2009); EN 1993-1-1 (CEN 2005b)], is admitted to simplify this design phase without excessive or unsafe approximations.

It appears hence of fundamental importance to evaluate α_{cr} or, equivalently, V_{cr} as accurately as possible. Usually, designers execute an initial buckling analysis under the most severe load conditions to select the method of analysis.

Very frequently, software programs, which are used in designer's offices, are able to predict only the flexural buckling load ($N_{cr,F}$) when the actual one should be the flexural torsional ($N_{cr,FT}$). As a consequence, relevant errors for the selection of methods of analysis are expected, owing to the absence of any attention to warping effects and the flexural-torsional buckling phenomena.

The choice of the method of analysis is critical to evaluate the actual degree of safety of the rack because the values of the set of displacements, internal forces, and moments strictly depend on the type of elastic analysis, i.e., first order, simplified second order, or second order, as shown by Bernuzzi et al. (2014b). To better explain this concept, a reference can be made to the uprights (Fig. 3) on which the present study is based, which were considered, for this purpose, as isolated members. Both $N_{cr,F}$, which is the minimum

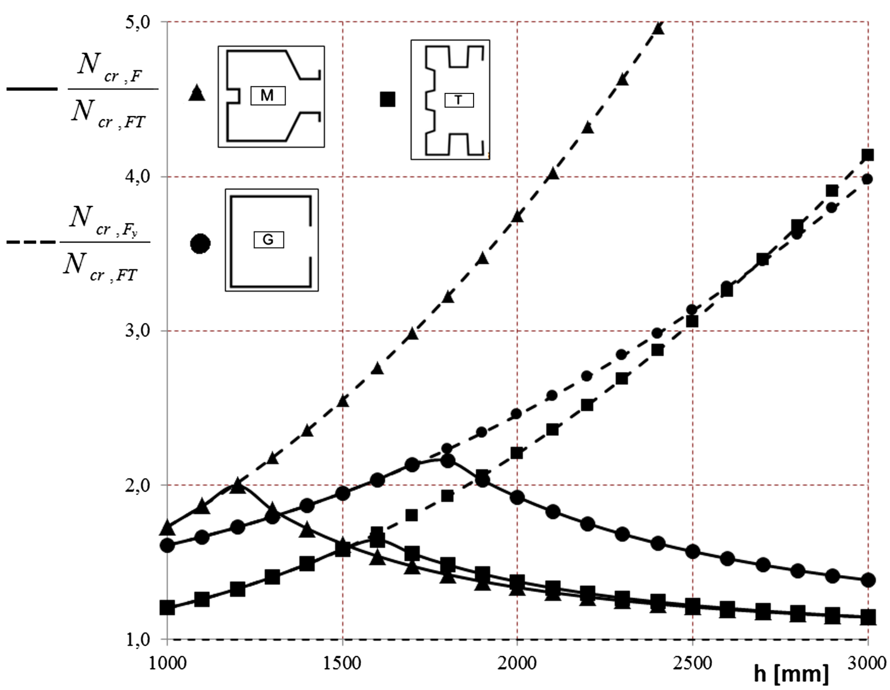

Fig. 6. $(N_{cr,F}/N_{cr,FT}) - h$ and $(N_{cr,Fy}/N_{cr,FT}) - h$ relationships for considered uprights

between the flexural buckling load about the x- and y-axes ($N_{\mathrm{cr},Fx}$ and $N_{\mathrm{cr},Fy}$, respectively), and $N_{\mathrm{cr,FT}}$ can be evaluated by either using the well-established theoretical approaches (Timoshenko and Gere 1961) or applying the *Śiva* buckling analyses. To allow comparison between the behavior of these isolated uprights with one of the uprights in the rack frames, the effective length for flexural buckling in the cross-aisle directions has been assumed constant and equal to the panel height (h_u) shown in Fig. 4 and the torsional one equal to $0.7h_u$, in accordance with the suggestions of European provisions [EN 15512 (CEN 2009)]. As an example of the importance of a correct assessment of the buckling load, Fig. 6 can be considered, where the ratio $N_{\mathrm{cr},F}/N_{\mathrm{cr,FT}}$ is plotted versus the effective length (h) for flexural buckling in the downaisle direction, which is represented by the solid lines. The dashed lines plot the $N_{\mathrm{cr},Fy}/N_{\mathrm{cr,FT}}$ ratio, which indicates when the flexural buckling in the cross-aisle direction is dominant to the one in the downaisle direction. The range of values of h has been selected to represent the most significant cases for routine rack design, which is related to both braced and unbraced racks in the downaisle direction. The trend of all the plotted curves is quite similar. It can be observed that

- Flexural-torsional buckling always occurs independently on the cross section upright or on the value of the effective length.
- For the lowest values of the effective length h, flexural buckling is governed by the cross-aisle direction; otherwise, flexural buckling is governed by the downaisle direction.
- The numerical values of the $N_{\mathrm{cr},Fy}/N_{\mathrm{cr,FT}}$ ratio are significantly greater than unity, confirming the nonnegligible importance of the coupling between flexure and torsion, which is up to 2 for *M_* and *G_* uprights and up to 1.8 for the *M_* uprights, and underlining at the same time the need for a correct choice of the analysis method to avoid significant errors.

From a practical point of view, a direct FE buckling analysis appears to be very convenient for design and, in the case of racks or more in general when the members present a singly symmetric cross section, the use of a seven-DOF beam element formulation is strongly recommended. Hand calculations are admitted. An approximate equation, strictly deriving from Horne's method (superscript H) (Horne 1975) is also recommended by EN 15512 (CEN 2009) and AS 4084 (Australian Standards 2012) to predict the critical buckling load or similarly the buckling load multiplier, respectively, as

$$V_{\mathrm{cr}}^{H} = \frac{\phi}{\phi_{\max}} V_{\mathrm{Ed}} \tag{5a}$$

$$\alpha_{\mathrm{cr}}^{H} = \frac{\phi}{\phi_{\max}} \tag{5b}$$

where ϕ = frame imperfection defined in terms of out of plumb of the uprights; and $\phi_{\max}$ = largest value of the sway index ϕ_s of any story (interstory drift) expressed as

$$\phi_s = (\delta_U - \delta_L)/h_{\mathrm{LL}} \tag{6}$$

where h_{LL} = story height; and δ_U and δ_L = horizontal deflection at the top and bottom of the story, respectively.

Numerical Applications

The aforementioned approach to predict the critical load multiplier α_{cr} has been applied to all of the considered racks. Owing to the presence of both six- and seven-DOF beam formulations in the FE analysis software *Śiva*, the values of elastic critical load multipliers α_{cr} associated with both beam formulations have been at first directly evaluated through a buckling analysis, which is identified in the following as α_{cr}^{6} and α_{cr}^{7}, respectively. The first term is related to the traditional routine rack design, which also neglects warping if singly symmetric cross section members are used. The term α_{cr}^{7} is related to the use of more appropriate design tools for open singly symmetric cross sections (Fig. 3), which require consideration of Wagner's constants and shear center eccentricity. To single out the warping influence on the overall buckling frame response, reference can be hence made to the $\alpha_{\mathrm{cr}}^{6}/\alpha_{\mathrm{cr}}^{7}$ ratio presented in Table 3 for all of the considered racks. Furthermore, Fig. 7 plots this ratio versus the nondimensional beam-to-column joint stiffness, $\rho_{j,\mathrm{btc}}$. Hence

- The $\alpha_{\mathrm{cr}}^{6}/\alpha_{\mathrm{cr}}^{7}$ ratio is always greater than unity, up to 1.18, underlining the nonnegligible influence of warping effects. This

Table 3. Influence of the Warping Effects on the Accuracy of Horne's Method

		$\rho_{j,\mathrm{base}} = 0.15$			$\rho_{j,\mathrm{base}} = 0.30$			$\rho_{j,\mathrm{base}} = 0.45$		
Racks	$\rho_{j,\mathrm{btc}}$	$\frac{\alpha_{\mathrm{cr}}^{6}}{\alpha_{\mathrm{cr}}^{7}}$	$\frac{\alpha_{\mathrm{cr}}^{6-H}}{\alpha_{\mathrm{cr}}^{7}}$	$\frac{\alpha_{\mathrm{cr}}^{7-H}}{\alpha_{\mathrm{cr}}^{7}}$	$\frac{\alpha_{\mathrm{cr}}^{6}}{\alpha_{\mathrm{cr}}^{7}}$	$\frac{\alpha_{\mathrm{cr}}^{6-H}}{\alpha_{\mathrm{cr}}^{7}}$	$\frac{\alpha_{\mathrm{cr}}^{7-H}}{\alpha_{\mathrm{cr}}^{7}}$	$\frac{\alpha_{\mathrm{cr}}^{6}}{\alpha_{\mathrm{cr}}^{7}}$	$\frac{\alpha_{\mathrm{cr}}^{6-H}}{\alpha_{\mathrm{cr}}^{7}}$	$\frac{\alpha_{\mathrm{cr}}^{7-H}}{\alpha_{\mathrm{cr}}^{7}}$
*M*_4	0.5	1.01	0.88	0.87	1.02	0.88	0.87	1.01	0.88	0.87
	1.0	1.03	0.92	0.89	1.03	0.90	0.87	1.04	0.90	0.87
	1.5	1.04	0.96	0.91	1.05	0.93	0.89	1.04	0.93	0.88
	2.0	1.05	1.01	0.94	1.05	0.97	0.90	1.06	0.96	0.90
	3.5	1.06	1.03	0.97	1.07	1.05	0.95	1.08	1.04	0.94
	5.0	1.07	1.02	0.96	1.08	1.08	0.98	1.09	1.09	0.96
	7.0	1.07	1.02	0.95	1.09	1.08	1.00	1.10	1.11	0.99
	10.0	1.07	1.03	0.95	1.09	1.08	0.99	1.10	1.11	1.02
*M*_5	0.5	1.01	0.89	0.88	1.01	0.90	0.88	1.00	0.89	0.87
	1.0	1.02	0.90	0.87	1.03	0.92	0.87	1.03	0.90	0.87
	1.5	1.04	0.93	0.88	1.05	0.93	0.88	1.05	0.92	0.88
	2.0	1.05	0.95	0.89	1.06	0.95	0.88	1.06	0.95	0.88
	3.5	1.08	1.01	0.93	1.09	1.04	0.91	1.10	1.03	0.91
	5.0	1.09	0.99	0.97	1.12	1.09	0.94	1.12	1.10	0.93
	7.0	1.10	0.98	0.96	1.13	1.06	0.96	1.14	1.11	0.96
	10.0	1.10	1.03	0.95	1.14	1.05	0.99	1.16	1.09	0.98
*G*_3	0.5	1.01	0.90	0.89	1.01	0.89	0.89	1.01	0.89	0.89
	1.0	1.03	0.91	0.89	1.03	0.88	0.88	1.03	0.90	0.88
	1.5	1.04	0.94	0.91	1.04	0.93	0.89	1.05	0.92	0.89
	2.0	1.05	0.98	0.93	1.06	0.95	0.90	1.06	0.94	0.90
	3.5	1.07	1.06	0.97	1.09	1.02	0.94	1.09	1.01	0.93
	5.0	1.09	1.05	1.00	1.11	1.08	0.97	1.12	1.06	0.96
	7.0	1.10	1.05	0.98	1.12	1.13	1.00	1.14	1.12	0.99
	10.0	1.11	1.05	0.97	1.14	1.13	1.03	1.16	1.17	1.02
*G*_4	0.5	1.04	0.93	0.89	1.02	0.91	0.89	1.02	0.90	0.84
	1.0	1.06	0.93	0.89	1.04	0.92	0.89	1.04	0.92	0.89
	1.5	1.07	0.94	0.89	1.06	0.92	0.88	1.05	0.92	0.88
	2.0	1.09	0.96	0.88	1.07	0.94	0.89	1.07	0.93	0.88
	3.5	1.12	1.03	0.93	1.11	0.99	0.84	1.10	0.98	0.76
	5.0	1.14	1.09	0.89	1.13	1.04	0.92	1.13	1.03	0.92
	7.0	1.16	1.13	0.98	1.16	1.09	0.95	1.16	1.08	0.80
	10.0	1.18	1.12	0.96	1.18	1.16	0.97	1.18	1.14	0.96
*T*_3	0.5	1.02	0.91	0.88	1.03	0.90	0.87	1.03	0.90	0.87
	1.0	1.03	0.95	0.92	1.03	0.92	0.89	1.03	0.92	0.89
	1.5	1.03	0.99	0.96	1.03	0.96	0.92	1.04	0.95	0.91
	2.0	1.04	1.02	0.94	1.04	0.99	0.94	1.05	0.97	0.92
	3.5	1.05	1.01	0.91	1.05	1.06	0.96	1.05	1.04	0.98
	5.0	1.05	1.01	0.91	1.06	1.06	0.94	1.06	1.01	0.97
	7.0	1.06	1.02	0.91	1.06	1.06	0.94	1.07	1.08	0.96
	10.0	1.06	1.02	0.95	1.07	1.07	0.94	1.07	1.09	0.96
*T*_4	0.5	1.03	0.90	0.87	1.03	0.90	0.87	1.03	0.90	0.87
	1.0	1.03	0.90	0.87	1.03	0.89	0.86	1.03	0.89	0.86
	1.5	1.04	0.93	0.90	1.04	0.91	0.88	1.04	0.91	0.87
	2.0	1.03	0.95	0.92	1.04	0.93	0.89	1.04	0.92	0.88
	3.5	1.04	1.01	0.97	1.05	0.98	0.93	1.05	0.97	0.92
	5.0	1.04	1.00	0.96	1.05	1.03	0.97	1.06	1.01	0.95
	7.0	1.05	0.99	0.95	1.06	1.05	1.00	1.06	1.05	0.98
	10.0	1.05	0.98	0.95	1.06	1.04	1.00	1.07	1.07	1.02

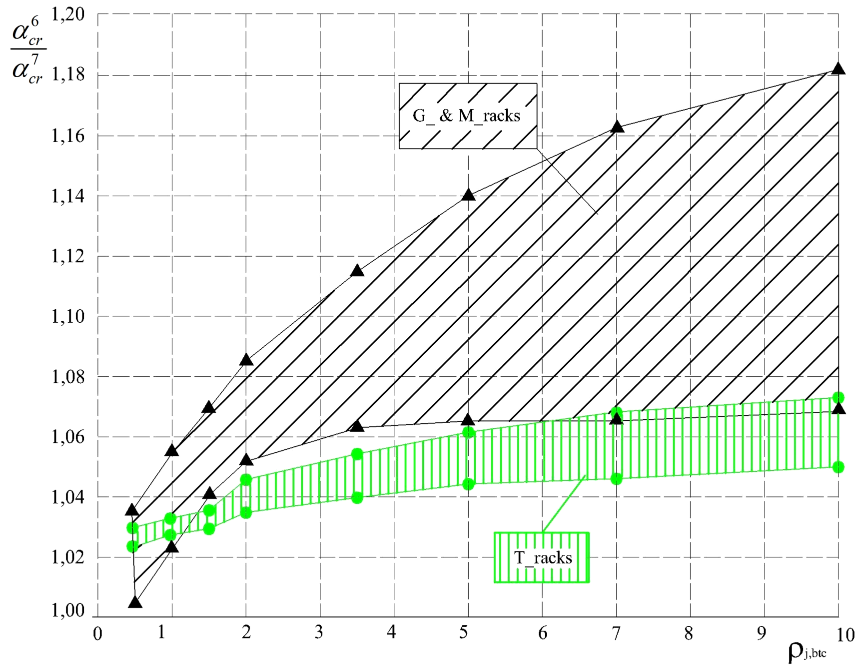

Fig. 7. Influence of warping on critical load multipliers for considered racks

influence is only slightly lower for the T_3 and T_4 racks, and the six-DOF overestimation is never greater than 7%.

- By increasing the degree of stiffness of the beam-to-column joints, this ratio also increases. The trend of the $\alpha_{\text{cr}}^6/\alpha_{\text{cr}}^7$-$\rho_{j,\text{btc}}$ relationships is similar for the $M\_$ and $G\_$ racks, whereas for the $T_$racks, a quite constant branch can be observed for the greatest values of $\rho_{j,\text{btc}}$.
- The $\alpha_{\text{cr}}^6/\alpha_{\text{cr}}^7$ ratio is moderately influenced for the $G\_$ and $M_$racks and also by the stiffness of the base-plate connections. By increasing $\rho_{j,\text{base}}$, the ratio slightly increases, especially for the greatest value of $\rho_{j,\text{btc}}$, whereas for $T_$racks, it is practically independent of the value of the base-plate stiffness.

Furthermore, Fig. 8 plots the frequency and cumulated relative frequency of the $\alpha_{\text{cr}}^6/\alpha_{\text{cr}}^7$ ratio for all of the considered racks. A nonnegligible concentration of data can be noted in the range of 1.02–1.10, and the 95% fractile value of the cumulated distribution is 1.154. Moreover, it should be pointed out that despite this the differences between α_{cr}^6 and α_{cr}^7 are not high, and remarkable differences can be noted in the set of internal forces and moments, as discussed by Bernuzzi et al. (2014a).

The maximum sway index ϕ_{max} has been evaluated by means of a first-order elastic analysis. Eq. (5*b*) has used this index to predict the elastic critical load multipliers α_{cr}^{6-H} and α_{cr}^{7-H}, adopting the set of horizontal displacements obtained using the six- and seven-DOF FE beam formulation, respectively. In Table 3, the ratios $\alpha_{\text{cr}}^{6-H}/\alpha_{\text{cr}}^7$ and $\alpha_{\text{cr}}^{7-H}/\alpha_{\text{cr}}^7$ are presented to allow a direct appraisal of the level of accuracy of Horne's equation and quantify the errors associated when warping effects are neglected at the same time. It appears that

- The use of the set of six-DOF FE displacements leads to a moderate underestimation of α_{cr}^7 of up to 12% in the case of very flexible racks, i.e., for the lowest values of $\rho_{j,\text{btc}}$ and $\rho_{j,\text{base}}$. Otherwise, the elastic critical load multiplier is overestimated for the $M\_$ and $G_$racks (up to 11 and 17%, respectively).
- In the case of the $T_$racks, owing to the more limited influence of the warping effects, because of the relevant differences between second moments of area to the lower value of the effective length for torsional buckling, the overestimation of α_{cr} is more limited and not greater than 9%.
- The set of seven-DOF displacements allows a more accurate appraisal of α_{cr} for design purposes, reducing the overestimation of α_{cr} significantly. The multiplier α_{cr}^{6-H} is always greater than α_{cr}^{7-H}, and the difference increases with the increase of beam-to column joint stiffness ($\rho_{j,\text{btc}}$).
- The $\alpha_{\text{cr}}^{7-H}/\alpha_{\text{cr}}^7$ ratio is generally lower than unity (not lower than 0.84), with a very limited number of exceptions; however, it is never greater than 1.02.

Fig. 9 shows the distribution of the relative frequencies of the $\alpha_{\text{cr}}^{6-H}/\alpha_{\text{cr}}^7$ and $\alpha_{\text{cr}}^{7-H}/\alpha_{\text{cr}}^7$ ratios, confirming that the use of α_{cr}^{7-H} should result in great interest for practical design, rarely leading to a slight overestimation of α_{cr}^7 and with an important concentration of data in the range of 0.89–0.98; otherwise, as previously discussed, traditional six-DOF formulations lead to a concentration of data between 0.95 and 1.15 and the overestimation of the actual buckling multiplier (α_{cr}^7) produces an unsafe design. Fig. 10 presents the distributions of the associated cumulated frequencies, where the 95% fractile values are indicated by solid lines. These fractile values can be directly used as safety factor γ^{k-H} to more correctly approximate the value of the elastic critical load multiplier of the frame in accordance with the philosophy of limit state design [EN 1990 (CEN 2005a)]. In particular, if a buckling analysis is avoided or it is necessary to quickly check the accuracy of the FE buckling load multiplier, reference should be made to the following equation:

$$\alpha_{\text{cr}}^7 = \frac{\alpha_{\text{cr}}^{k-H}}{\gamma_{\text{cr}}^{k-H}} \tag{7}$$

where the value of γ_{cr}^{k-H} has been obtained from reanalysis of the data in the table. From the cases considered in the present study, it results in $\gamma_{\text{cr}}^{6-H} = 1.123$ when associated with α_{cr}^{6-H}, i.e., if the six-DOF set of displacement is used; otherwise, if reference is made to α_{cr}^{7-H}, i.e., the multiplier based on the seven-DOF set of displacements, $\gamma_{\text{cr}}^{7-H} = 1.00$ can be used, i.e., in practice, no correction of Horne's multiplier is required if the warping presence is considered to obtain the set of displacements.

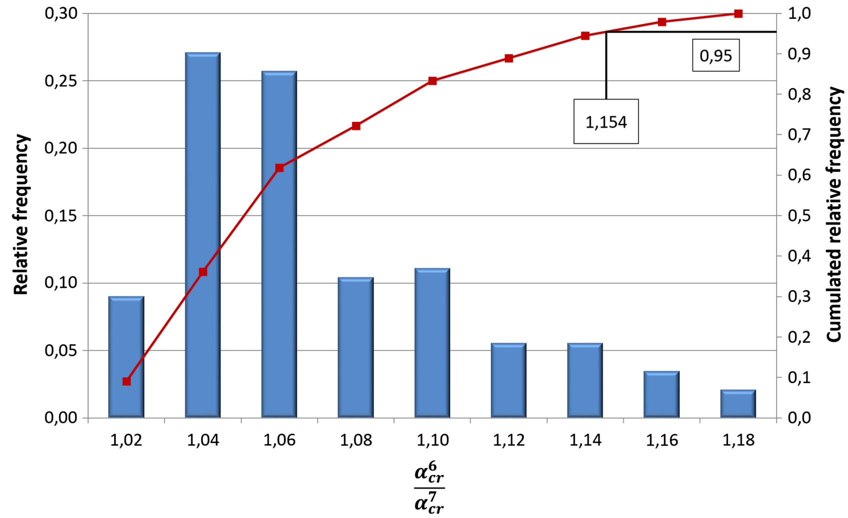

Fig. 8. Frequency and cumulated relative frequency for $\alpha_{\mathrm{cr}}^{6}/\alpha_{\mathrm{cr}}^{7}$ ratio

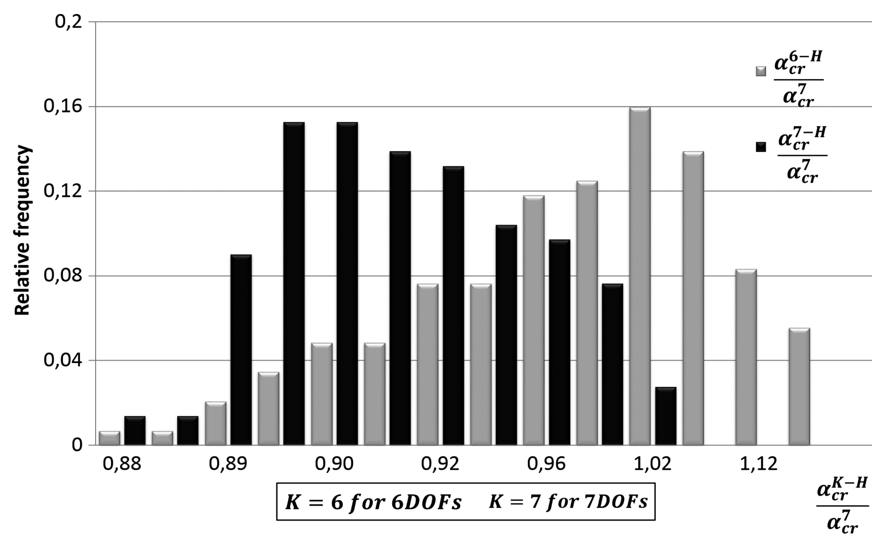

Fig. 9. Distribution of relative frequency of $\alpha_{\mathrm{cr}}^{6-H}/\alpha_{\mathrm{cr}}^{7}$ and $\alpha_{\mathrm{cr}}^{7-H}/\alpha_{\mathrm{cr}}^{7}$ for all considered racks

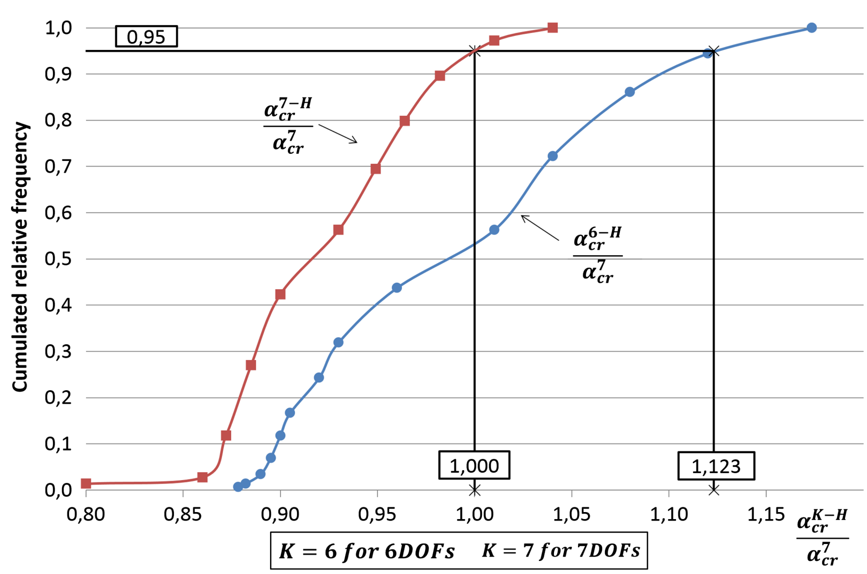

Fig. 10. Distribution of cumulated relative frequency of $\alpha_{\mathrm{cr}}^{6-H}/\alpha_{\mathrm{cr}}^{7}$ and $\alpha_{\mathrm{cr}}^{7-H}/\alpha_{\mathrm{cr}}^{7}$ for all considered racks

Concluding Remarks

The uprights (vertical elements) of steel storage pallet racks generally have an open singly symmetric cross section, which is often characterized by the noncoincidence between the shear center and centroid. With reference to a member having a cross section similar to those presented in Fig. 3, Wagner's effects, warping deformations, and the coupling between flexure and torsion play a fundamental role in the behavior of racks. As a consequence, their design necessarily requires advanced FE structural analysis programs and also inclusion of the seventh DOF (warping). Simplified approaches, which are of fundamental importance for preliminary design and a qualitative check of the reliability of the design procedures, have been validated in the past with reference to the more traditional steel-framed structures made by doubly symmetric cross section members. This first part of the two-part paper has discussed their direct extension to racks, where research outcomes of interest for static design have been discussed on the basis of an extensive numerical analysis regarding typical medium-rise racks unbraced in the downaisle direction. Prediction of the elastic critical load multiplier for the sway mode made (α_{cr}^7) through the traditional Horne's approach should only be used for racks if the interstory drift takes into account warping influence, i.e., the set of first-order elastic displacements has been obtained by using seven-DOF FE beam element formulations. It has been shown that α_{cr}^7 is generally never greater than the one numerically obtained by Horne's method and its errors are modest, confirming its convenience for practical design. Otherwise, if a more traditional six-DOF beam formulation is used, in several cases, α_{cr}^6 is significantly overestimated (up to approximately 25%), especially for higher values of the beam-to-column joint rotational stiffness, hence leading to an excessively conservative rack design. In these cases, a suitable safety factor accounting for nonappropriate FE beam formulation should be used for routine design.

Appendix. Elastic Stiffness Matrix for a Seven-DOF Beam Element

Let j and k denote the two nodes of the generic beam element. The governing matrix displacement equations can be written in a general form, which is valid with reference to both elastic $[K]_E$ and geometric $[K]_G$ stiffness matrices, such as

$$\begin{bmatrix} [K]_{jj} & [K]_{jk} \\ [K]_{kj} & [K]_{kk} \end{bmatrix} \begin{bmatrix} \{u\}_j \\ \{u\}_k \end{bmatrix} = \begin{bmatrix} \{f\}_j \\ \{f\}_k \end{bmatrix} \tag{8}$$

With reference to the more general case of seven-DOF formulation, the nodal displacement $\{u\}_j$ and $\{u\}_k$ and the associate force vectors $\{f\}_j$ and $\{f\}_k$ can be expressed [Fig. 2(b)], respectively, as

$$\{u\}_j = \begin{bmatrix} w_O \\ u_S \\ v_S \\ \varphi_z \\ \varphi_x \\ \varphi_y \\ (\theta) \end{bmatrix} \tag{9a}$$

$$\{f\}_j = \begin{bmatrix} N \\ F_x \\ F_y \\ M_t \\ M_x \\ M_y \\ (B) \end{bmatrix} \tag{9b}$$

The presence of the terms θ (warping) and B (bimoment) is only associated with the case of FE beam formulations, which also include the seventh DOF. Because it also results from Chen and Atsuta (1977), these formulations are very complex, especially for what concerns the definition of the geometric stiffness matrix $[K]^G$; otherwise, modifications required to obtain the seven-DOF FE formulation starting from the six DOF one are quite limited for the elastic matrix $[K]^E$. With reference to a beam element of length L_b by considering its area (A), second moments of area (I_x and I_y) along principal axes, and uniform and nonuniform torsional constants (I_t and I_w, respectively) and assuming that E and G represent Young's and shear modulus, respectively, the stiffness elastic submatrices $[K]_{jj}^E$ or, equivalently, $[K]_{kk}^E$ and $[K]_{jk}^E$ or $[K]_{kj}^E$ are defined as

$$[K]_{jj}^E = \begin{bmatrix} \frac{EA}{L_b} & 0 & 0 & 0 & 0 & 0 & 0 \\ & \frac{12EI_y}{L_b^3} & 0 & 0 & 0 & \frac{6EI_y}{L_b^2} & 0 \\ & & \frac{12EI_x}{L_b^3} & 0 & -\frac{6EI_x}{L_b^2} & 0 & 0 \\ & & & \frac{GI_t}{L_b} + \left(\frac{12EI_w}{L_b^3} + \frac{1}{5}\frac{GI_t}{L_b}\right) & 0 & 0 & \left(\frac{6EI_w}{L_b^2} + \frac{3}{30}GI_t\right) \\ & \text{Symmetric} & & & \frac{4EI_x}{L_b} & 0 & 0 \\ & & & & & \frac{4EI_y}{L_b} & 0 \\ & & & & & & \left(\frac{4\mathrm{EI}_w}{L_b} + \frac{4}{30}GI_tL_b\right) \end{bmatrix} \tag{10a}$$

$$[K]_{jk}^{E} = \begin{bmatrix} -\frac{EA}{L_b} & 0 & 0 & 0 & 0 & 0 & 0 \\ 0 & -\frac{12EI_y}{L_b^3} & 0 & 0 & 0 & \frac{6EI_y}{L_b^2} & 0 \\ 0 & 0 & -\frac{12EI_x}{L_b^3} & 0 & -\frac{6EI_x}{L_b^2} & 0 & 0 \\ 0 & 0 & 0 & -\frac{GI_t}{L_b} - \left(\frac{12EI_w}{L_b^3} + \frac{1}{5}\frac{GI_t}{L_b}\right) & 0 & 0 & \left(\frac{6EI_w}{L_b^2} + \frac{3}{30}GI_t\right) \\ 0 & 0 & \frac{6EI_x}{L_b^2} & 0 & \frac{2EI_x}{L_b} & 0 & 0 \\ 0 & -\frac{6EI_y}{L_b^2} & 0 & 0 & 0 & \frac{2EI_y}{L_b} & 0 \\ 0 & 0 & 0 & \left(-\frac{6EI_w}{L_b^2} - \frac{3}{30}GI_t\right) & 0 & 0 & \left(\frac{2EI_w}{L_b} - \frac{1}{30}GI_tL_b\right) \end{bmatrix} \quad (10b)$$

The terms between brackets are related to the sole formulations, including the seventh DOF (warping), which also directly influences the terms associated with uniform torsion, i.e., the term (4.4) in the submatrices Eqs. (10*a*) and (10*b*). The classical six-DOF FE beam formulations are characterized by the presence of the term GI_t/L_b in the elastic stiffness matrix $[K]^E$. In the case of seven-DOF formulation, the contribution $[(12EI_w/L_b^3)+(1/5)(GI_t/L_b)]$ has to be directly added for $[K]_{jj}^E$ in submatrix Eq. (10*a*) or subtracted for $[K]_{jj}^E$ in submatrix Eq. (10*b*) to GI_t/L_b.

Furthermore, with reference to the geometric stiffness matrix $[K]^G$, the traditional six-DOF FE beam formulations implemented in the most common commercial analysis packages require knowledge of the sole value of the internal axial load N, despite the improvements proposed in the literature. As an example, McGuire (1992) and Teh and Clarke (1998) suggested also including bending moments in the geometric stiffness matrix. In the case of beam formulations, including warping, bending moments (M_x and M_y), torsional moment (M_t), bimoment (B), and shear actions (F_x and F_y) also significantly contribute to form the geometric stiffness $[K]^G$. The terms of $[K]^G$ also strictly depend on the distance between the load application point and shear center.

As already discussed, only the presence of the seventh DOF allows correct estimation of both frame displacements and the set of internal forces and moments, which significantly influence the local state of stress of upright cross sections. Furthermore, these formulations take into account the coupling between flexure and torsion are the ones, as clearly discussed by C. Bernuzzi and A. Gobetti ("An innovative finite element formulation for analysis of beam element with thin-walled mono-symmetric section," submitted, *Costruzioni Metalliche*) and Bernuzzi et al. (2014a, b, 2015a, b), which is capable of also directly capturing the overall flexural-torsional buckling of the frame and isolated columns, beams, and beam columns.

Notation

The following symbols are used in this paper:

A = cross-sectional area;
B = bimoment;
d = eccentricity between centroid and middle line of web;
E = Young's modulus;
F = shear force, horizontal force;
f = force;
G = shear modulus;
H = height;
h = height;
I = second moment of area;
K = stiffness matrix;
L = length;
M = moment, mass matrix;
N = axial force;
O = position of the centroid;
S = beam-to-column joint stiffness, base-plate joint stiffness, and position of shear center;
u = displacement along x-axis;
V = vertical load;
v = displacement along y-axis;
W = section modulus;
w = displacement along z-axis;
x = symmetry axis of the cross section and distance between centroid and shear center;
y = nonsymmetry axis of cross section;
z = longitudinal axis of beam;
α = load multiplier;
δ = horizontal deflection;
ϕ = out of plumb;
γ = safety factor;
φ = rotation;
θ = warping function; and
ρ = radius gyrator of inertia, adimensional stiffness.

Subscripts

b = beam;
base = base-plate connection;
btc = beam-to-column connection;
cr = critical;
Ed = design value;
F = flexural buckling;
FT = flexural-torsional buckling;
I = i-esim;
inf = lower value of the section modulus;
j = initial node of beam element, joint;
k = end node of beam element;
L = lower;

LL = load level;
max = maximum;
O = position of centroid;
S = position of shear center, sway index;
sup = upper value of section modulus;
t = Saint Venant's torsion;
tot = total;
U = upper;
u = upright;
w = warping;
x = symmetry axis of cross section;
y = non symmetry axis of cross section; and
z = longitudinal axis of beam element.

Superscripts

E = elastic stiffness matrix;
EC3-LB = lower bound of semirigid domain value;
EC3-UB = upper bound of semirigid domain value;
G = geometric stiffness matrix;
H = Horne's method;
K = index used to identify six- or seven-DOF FE beam formulation;
6 = analysis with beam element formulation having six DOFs per node; and
7 = analysis with beam element formulation having seven DOFs per node.

References

Australian Standards. (2012). "Steel storage racking." *AS 4084*, Sydney, Australia.

Bajoria, K. M., Sangle, K. K., and Talicotti, R. S. (2010). "Modal analysis of cold-formed pallet rack structures with semi-rigid connections." *J. Constr. Steel Res.*, 66(3), 428–441.

Baldassino, N., and Bernuzzi, C. (2000). "Analysis and behaviour of steel storage pallet racks." *Thin Walled Struct.*, 37(4), 277–304.

Baldassino, N., and Zandonini, R. (2011). "Design by testing of industrial racks." *Adv. Steel Constr.*, 7(1), 27–47.

Bathe, K., and Wilson, E. L. (1976). *Numerical methods in finite element analysis*, Prentice-Hall, NJ.

Bathe, K. J., Wilson, E. L., and Iding, R. H. (1978). "NONSAP-finite element calculation for nonlinear static and dynamic analysis of complex structures." Structural Engineering Laboratory, Univ. of California, Berkeley, CA.

Bernuzzi, C., and Gobetti, A. (2014). "An innovative finite element formulation for analysis of beam element with thin-walled mono-symmetric section." *Costruzioni Metalliche*, ACAI, Milano, Italy.

Bernuzzi, C., Gobetti, A., Gabbianelli, G., and Simoncelli, M. (2015a). "Simplified approaches to design medium-rise unbraced steel storage pallet racks. II: Fundamental period estimates." *J. Struct. Eng.*, 10.1061/(ASCE)ST.1943-541X.0001278, 04015037.

Bernuzzi, C., Gobetti, A., Gabbianelli, G., and Simoncelli, M. (2015b). "Unbraced pallet rack design in accordance with European practice—Part 2: Essential verification checks." *Thin Walled Struct.*, 86, 208–229.

Bernuzzi, C., Gobetti, A., Gabbianelli, G., and Simoncelli, M. (2014a). "Warping influence on the resistance of uprights in steel storage pallet racks." *J. Constr. Steel Res.*, 101, 224–241.

Bernuzzi, C., Pieri, A., and Squadrito, V. (2014b). "Warping influence on the static design of unbraced steel storage pallet racks." *Thin Walled Struct.*, 79, 71–82.

CEN (European Committee for Standardization). (2005a). "Eurocode 0: Basis of structural design." *EN 1990*, Brussels, Belgium.

CEN (European Committee for Standardization). (2005b). "Eurocode 3: Design of steel structures—Part 1-1: General rules and rules for buildings." *EN 1993-1-1*, Brussels, Belgium.

CEN (European Committee for Standardization). (2005c). "Eurocode 3: Design of steel structures—Part 1-8: Design of joints." *EN 1993-1-8*, Brussels, Belgium.

CEN (European Committee for Standardization). (2009). "Steel static storage systems—Adjustable pallet racking systems—Principles for structural design." *EN 15512*, Brussels, Belgium 137.

Chen, W. F., and Atsuta, T. (1977). *Theory of beam-columns, Vol. 2: Space behaviour and design*, Mc-Graw Hill, New York.

ConSteel Solutions. (2010). "Finite-element-program." ⟨http://www.consteel.hu⟩ (May 8, 2014).

Dinis, P. B., Young, B., and Camotin, D. (2013). "Local-distortional interaction in cold-formed steel rack-section column." *Thin Walled Struct.*, 81, 185–194.

Filialtrault, A., Higgins, P. S., and Wanitkortkul, A. (2006). "Experimental stiffness and seismic response of pallet-type steel storage rack connectors." *Pract. Period. Struct. Des. Constr.*, 10.1061/(ASCE)1084-0680(2006)11:3(161), 161–170.

Gilbert, B. P., and Rasmussen, K. J. R. (2012). "Drive-in steel storage racks. I: Stiffness test and 3D load transfer mechanisms." *J. Struct. Eng.*, 10.1061/(ASCE)ST.1943-541X.0000449, 135–147.

Godley, M. H. R. (1991). "Storage racking." Chapter 11, *Design of cold formed steel members*, Rhodes, ed., Elsevier Applied Science, London, 361–398.

Hibbit, Karlsson and Sorensen. (2006). *Abaqus 6.8 user's manual*, Providence, RI.

Horne, M. R. (1975). "An approximate method for calculating the elastic critical loads of multi-storey plane frame." *Struct. Eng.*, 53(6), 242–248.

Hsiao, K. M., and Lin, W. Y. (2000). "A co-rotational formulation for thin-walled beams with mono-symmetric open sections." *Comput. Meth. Appl. Mech. Eng.*, 190(8), 1163–1185.

Hughes, T. J. R. (1987). *The finite element methods*, Prentice-Hall, NJ.

LS-DYNA [Computer software]. Livermore, CA, Livermore Software Technology Corporation.

McGuire, W. (1992). "Computer-aided analysis." *Constructional steel design—An international guide*, P. J. Dowling, J. E. Harding, and R. Bjorhovde, eds., Elsevier Applied Science, New York, 915–931.

RMI (Rack Manufacturers Institute). (2012). "Specification for the design, testing and utilization of industrial steel storage racks." *RMI MH 16.1: 2012*, Charlotte, NC, 59.

Sangle, K. K., Bajoria, K. M., and Talicotti, R. S. (2012). "Elastic stability analysis of cold-formed pallet rack structures with semi-rigid connections." *J. Constr. Steel Res.*, 71, 245–262.

Shafer, B. W. (2011). "Cold-formed steel structures around the world—A review of recent advances in applications, analysis and design." *Steel Constr.*, 4(3), 141–149.

SOFiSTiK. (2013). "The SOFiSTiK FEM packages." ⟨http://www.sofistik.com/en/⟩ (Dec. 1, 2013).

Teh, L. H., and Clarke, M. J. (1998). "Co-rotational and Lagrangian formulations for elastic three-dimensional beam finite elements." *J. Constr. Steel Res.*, 48(2–3), 123–144.

Teh, L. H., Hancock, G. J., and Clarke, M. J. (2004). "Analysis and design of double sided high-rise steel pallet rack frames." *J. Struct. Eng.*, 10.1061/(ASCE)0733-9445(2004)130:7(1011), 1011–1021.

Timoshenko, S. P., and Gere, J. M. (1961). *Theory of elastic stability*, 2nd Ed., McGraw Hill, New York.

Turkalj, G., Brnic, J., and Prpic-Orsic, J. (2003). "Large rotation analysis of elastic thin-walled beam-type structures using ESA approach." *Comput. Struct.*, 81(18–19), 1851–1864.

Vlasov, V. Z. (1961). *Thin walled elastic beams*, 2nd Ed., Israel Program for Scientific Transactions, Jerusalem, Israel.

Werkle, H. (2008). *Finite element in der Baustatik*, Vieweg, Braunschweig-Wiesbaden, Germany.